BIODIVERSITAS
Volume 25, Number 10, October 2024
Pages: 3555-3567

ISSN: 1412-033X
E-ISSN: 2085-4722
DOI: 10.13057/biodiv/d251017

LC-HRMS profiling, antibacterial activities, and in silico study of ethyl acetate extract from *Dracaena angustifolia* root bark

I WAYAN KARTA[1,2,♥], WARSITO WARSITO[3,♥♥], MASRURI MASRURI[3], I WAYAN MUDIANTA[4]

[1]Doctoral Program of Chemistry, Faculty of Mathematics and Natural Sciences, Universitas Brawijaya. Jl. Veteran, Malang 65145, East Java, Indonesia. Tel./Fax.: +62-341-575835, ♥email: iwayankarta@student.ub.ac.id

[2]Department of Medical Laboratory Technology, Politeknik Kesehatan Kemenkes Denpasar. Jl. Sanitasi No. 1, Denpasar 80224, Bali, Indonesia

[3]Department of Chemistry, Faculty of Mathematics and Natural Sciences, Universitas Brawijaya. Jl. Veteran, Malang 65145, East Java, Indonesia. Tel.: +62-812-3309-654, ♥♥email: warsitoub@ub.ac.id

[4]Department of Chemistry, Faculty of Mathematics and Natural Sciences, Universitas Pendidikan Ganesha. Jl. Udayana No. 11, Buleleng 81116, Bali, Indonesia

Manuscript received: 25 August 2024. Revision accepted: 11 October 2024.

Abstract. *Karta IW, Warsito W, Masruri M, Mudianta IW. 2024. LC-HRMS profiling, antibacterial activities, and in silico study of ethyl acetate extract from* Dracaena angustifolia *root bark. Biodiversitas 25: 3555-3567.* The escalating resistance of bacteria to conventional antibiotics has spurred new sources of exploration of natural antibacterial agents. This study aimed to unveil the antibacterial potential of *Dracaena angustifolia* Roxb. root bark extract through a comprehensive approach of in vitro assays, LC-HRMS analysis, in silico, and molecular dynamics simulations. The root bark, extracted with ethyl acetate, was identified using LC-HRMS and tested for antibacterial activity using the diffusion method. The extract demonstrated the ability to inhibit the growth of *Staphylococcus aureus*, *Enterococcus faecalis*, *Escherichia coli*, and *Salmonella typhi*. Of 37 annotated compounds, four (Arbutin, (-)-Caryophyllene oxide, Ruscoponticoside C, and Striatisporolide A) were predicted by PASS to exhibit antibacterial potential. Molecular docking revealed differences in the binding interactions between amino acid residues and ligands of the target protein (PDB ID: 3HUN). Ruscoponticoside C shares binding site similarities with the native ligand Ampicillioic acid. Molecular dynamics simulations showed that the ligand-protein complexes of Arbutin, Ruscoponticoside C, Striatisporolide A, and Ampicillioic acid were more stable compared to Chloramphenicol. This study suggests that this plant's root bark extract has potential as an antibacterial agent, inspiring further in-depth research into the isolation of its secondary metabolites and their potential impact on drug discovery.

Keywords: Antibacterial, *Dracaena angustifolia*, in silico, LC-HRMS, root bark

INTRODUCTION

The discovery of antibacterial agents from plants or herbs is significantly important for the medical field, especially given the increasing issue of bacterial resistance to conventional antibiotics. Medicinal plants provide abundant sources of bioactive compounds with diverse therapeutic potential. They provide a wealth of antimicrobial agents, with over 1,340 species documented for their antimicrobial properties and more than 30,000 plant-derived antimicrobial compounds identified (Ramata-Stunda et al. 2022; Masruri et al. 2024). Moreover, natural compounds frequently exhibit unique mechanisms of action capable of overcoming existing bacterial resistance, highlighting their antimicrobial activity, potential mechanisms, and chemical promise (Vaou et al. 2021). Researching and identifying new antibacterial compounds from plants enables the development of drugs that are not only more effective but also safer, reducing the reliance on synthetic antibiotics that often lead to harmful side effects. This discovery also promotes the sustainability of natural resources and creates opportunities for the development of environmentally friendly health products that are not only effective but also culturally accepted in various communities, fostering respect and consideration for diverse cultural practices.

Plants from the genus *Dracaena* have significant potential in ethnomedicine and as antimicrobial agents. The genus *Dracaena* includes over 120 recognized species, mostly distributed in Africa, Australia, India, and Southeast Asia (Babu and Prabhu 2024). Several *Dracaena* species are extensively utilized in various Asian traditional medicines due to their production of diverse secondary metabolites (Thu et al. 2020). These metabolites exhibit potent antimicrobial, antioxidant, analgesic, anti-inflammatory, antiproliferative, and cytotoxic activities (Thu et al. 2021; Ghalloo et al. 2022; Dewatisari and To'bungan 2024). One species of this plant genus utilized in ethnomedicine is *Dracaena angustifolia* Roxb. This plant has long been utilized in traditional medicine to treat various ailments (Yi et al. 2022). The leaves are employed in treating hypertension (Surayya et al. 2016), inflammation (Sakong et al. 2011), and jaundice (Dutta and Barooah 2021).The bark serves as a remedy for gastroenteritis (Huang et al. 2016) and fractures (Villanueva and Buot 2020). The roots are extensively used to treat leukemia (Banskota et al. 2003), digestive diseases (Hanh et al. 2021), and gastritis (Barua and Sonowal 2011). The root bark ethyl acetate extract contains flavonoids, tannins, saponins, phenolics, alkaloids, and terpenoids and exhibits high antioxidant activity (Karta et al. 2024). Owing to no research reporting

the antibacterial potential of the root bark of this plant, it is essential to conduct studies on the compound profiling and antibacterial activity of this extract to identify the most effective compounds and their mechanisms of action.

Liquid chromatography coupled with high-resolution mass spectrometry (LC-HRMS) is employed for the identification of secondary metabolites in diverse crude extracts (Aryal et al. 2021). This technique helps determine the structure of bioactive compounds through the analysis of retention time and accurate mass, thereby establishing a scientific basis for further research into the biological activity of the extract (Sasse and Rainer 2022). Once the predicted compounds in an extract are identified, an in silico (molecular docking) approach, a promising avenue in drug discovery, can be applied to assess the potential bioactivity of the compound and its interaction with the target protein (Pinzi and Rastelli 2019). This approach involves computer modeling and simulation, serving as a crucial tool in exploring interactions between bioactive compounds and molecular targets in bacteria (Breijyeh and Karaman 2023). This method not only accelerates the drug discovery process but also delivers valuable insights into the underlying mechanisms of action of antibacterial compounds (Abdallah et al. 2023). The primary objective of this research was to evaluate the antibacterial activity of the ethyl acetate extract derived from the root bark of *D. angustifolia*, profile its compounds using LC-HRMS, and model the interactions of bioactive compounds with bacterial targets through in silico studies, with the aim of developing natural antibacterial agents.

MATERIALS AND METHODS

Plant collection

Dracaena angustifolia root bark was collected in Ped Village, Bali, Indonesia, in May 2023 (Figure 1). The species has been identified at the Taxonomy, Structure, and Plant Development Laboratory, Department of Biology, Universitas Brawijaya, Indonesia (No. 0270/UN10.F09.42/10/2022).

Procedures

Extraction

The orange-colored root bark was washed under flowing water, dried in a hybrid room maintained at 40 to 50°C with a humidity level of 25%, and then ground into a powder with a moisture content of 4.009%. The powder was macerated with ethyl acetate (Merck, p.a., Germany) with a ratio of 1:8 (100 g: 800 mL) and soaked for 24 hours. Each mixture was filtered, and the filtrate was evaporated using a rotary evaporator (BUCHI R-300, Swiss) at 40°C, 150 mbar, resulting in the extract, which was stored in the refrigerator at 4°C until further analysis.

Antibacterial activity assay

The test bacteria of the extract were performed against pathogenic Gram-positive bacteria (*Staphylococcus aureus* ATCC 25923 and *Enterococcus faecalis* ATCC 29212) and then Gram-negative bacteria (*Escherichia coli* ATCC 25922 and *Salmonella typhi* ATCC19430). These bacteria were obtained as clinical isolates from the microbiology laboratory of the Department of Medical Laboratory Technology, Health Ministry Polytechnic Denpasar, Bali, Indonesia. The bacteria were stored on an inclined Luria-Bertani (LB) agar medium at 4°C (Fadana et al. 2023). Before the test, the bacteria were activated by subculturing in a suitable culture medium (LB) at 35°C for 24 h (ESCO IFA-110-8, Singapore). After incubation, the bacteria were suspended in Nutrient Broth (NB) within sterile test tubes, and their density was measured using a Densichek Plus densitometer (BIOSAN DEN-1B, Latvia) until it reached 0.5 McFarland (1-2×10^8 CFU/mL) (Balouiri et al. 2016). For each assay, each inoculum was smeared on a Petri dish with Mueller-Hinton Agar (MHA) (Oxoid, UK).

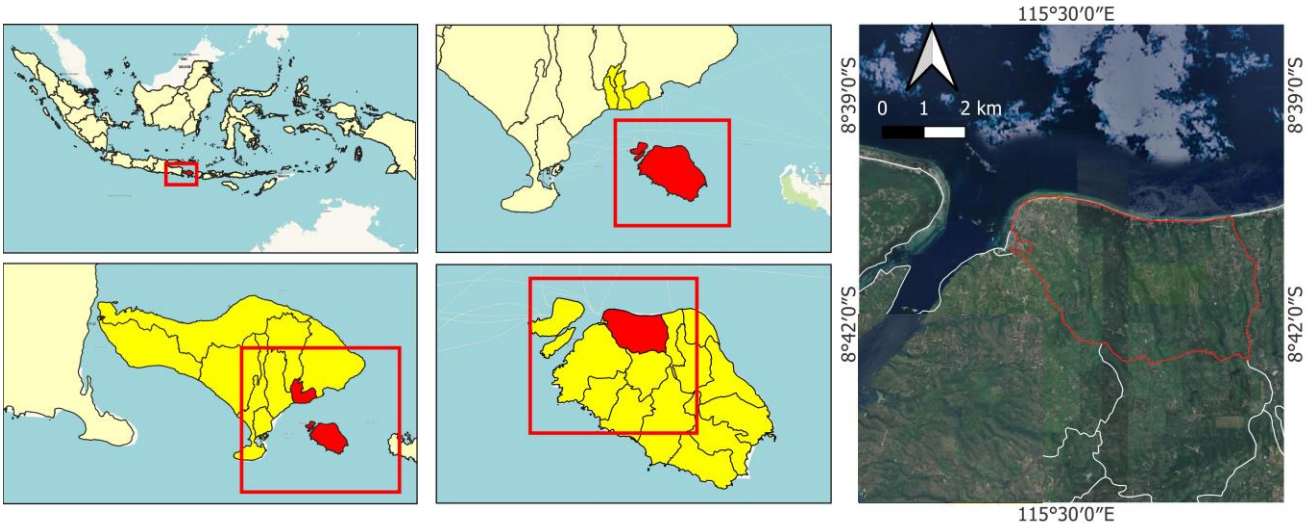

Figure 1. *Dracaena angustifolia* Roxb. root bark sampling location in Ped Village, Nusa Penida Sub-district, Klungkung, Bali, Indonesia

Antibacterial activity assay employed Kirby bauer disc diffusion method (Campos et al. 2022; Rustini et al. 2023), with slight modification. Each extract was dissolved in Dimethyl sulfoxide (DMSO) (Merk, Germany) with concentrations of 5%, 25%, and 25% and dripped as much as 30 µL on a sterile blank disc (Oxoid, UK). The positive control used Chloramphenicol (Oxoid, UK) at 30 µg/mL, while the negative control utilized DMSO dripped at 30 µL on a blank disk. Each disk was inoculated into a petri dish containing bacterial inoculum and incubated at 37°C for 24 hours, with each treatment plicated three times. Antibacterial activity was indicated by clear zones in the media (inhibition zone) and measured in millimeters.

LC-HRMS analysis

Screening of bioactive compounds was carried out on the ethyl acetate extract derived from the root bark of *D. angustifolia*, which had the best antibacterial activity. An examination was performed using liquid chromatography with a Thermo Scientific™ Vanquish™ UHPLC Binary Pump and Orbitrap high-resolution mass spectrometry utilizing a Thermo Scientific™ Q Exactive™ Hybrid Quadrupole-Orbitrap™ High-Resolution Mass Spectrometer. The liquid chromatography procedure utilized a Thermo Scientific™ Accucore™ Phenyl-Hexyl analytical column with dimensions of 100×2.1 mm ID × 2.6 µm. The mobile phases consisted of MS-grade water with 0.1% formic acid (A) and MS-grade methanol with 0.1% formic acid (B), following a gradient technique at a flow rate of 0.3 mL/min. Initially, mobile phase B was set at 5%, increased gradually to 90% over 16 minutes, maintained at 90% for 4 minutes, and then returned to the initial condition (5% B) by 25 minutes. The column temperature was maintained at 40°C, and the injection volume was 3 µL. Untargeted screening was performed using full MS/dd-MS2 acquisition mode in either positive ionization polarities/states. Nitrogen served as a sheath, auxiliary, and sweep gas at 32, 8, and 4 arbitrary units (AU), respectively. The spray voltage was set to 3.30 kV, the capillary temperature was maintained at 320°C, and the auxiliary gas heater temperature was adjusted to 30°C. The scan range spanned 66.7-1000 m/z, with a resolution of 70,000 for full MS and 17,500 for dd-MS2 in positive ionization modes. The system was controlled by XCalibur 4.4 software from Thermo Scientific, Bremen, Germany. The instruments underwent tuning and calibration weekly in ESI positive modes to maintain optimal and robust instrumental performance, using Thermo Scientific Pierce ESI ion calibration solutions (Waltham, MA). This ensured accuracy (<5 ppm) in mass measurement, ion transfer, ion isolation, and instrumental sensitivity throughout the analysis. The putative identification of the metabolites was conducted using the acquired mass spectra and analyzed with Compound Discoverer 3.2 software. The compounds were then examined for peak extraction using MzCloud and ChemSpider databases, with annotated masses ranging from -5 ppm to 5 ppm. Only chemicals with a complete MzCloud and ChemSpider match were selected for analysis. Each predicted compound was matched with various scientific articles on the genus *Dracaena* and natural product web servers, such as lotus.naturalproducts.net, coconut.naturalproducts.net, and www.knapsackfamily.com.

Target prediction and docking analysis

The compounds identified by LC-HRMS for docking were determined based on predicted biological activity using the PASS Online tool from the Way2Drug platform [Way2Drug.com©2011-2022, version 2.0, Moscow, Russia] (www.way2drug.com/passonline/, accessed on 16 June 2024). The PASS program classifies biological activity into 'active' (Pa) or 'inactive' (Pi), with estimated probabilities ranging from zero to one. The interpretation of Pa and Pi probabilities is as follows: (i) if Pa > Pi, the compound is likely considered active; (ii) if Pa >0.7, the compound is likely to exhibit biological activity and has a high probability of being an analog of a known pharmaceutical drug; (iii) if 0.5<Pa<0.7, the compound may have similar effects to the experimental one but with lower probability and is not similar to a known drug; (iv) if Pa<0.5, the compound does not match the experimental activity but, if confirmed by experimental data, could become a new subject for investigation (Mendonça et al. 2022). Compounds proceeding to the docking process are those with Pa>0.5.

The compounds' 3D structures were retrieved from the PubChem database (https://pubchem.ncbi.nlm.nih.gov/). The target protein structure 3HUN was retrieved from the Protein Data Bank (https://www.rcsb.org/) and prepared using UCSF Chimera (v.1.16) software (The Regents of the University of California) to remove water molecules (Gaona-López et al. 2024). The grid box coordinates used for docking the target protein 3HUN were set in Vina's search space with center coordinates X = -15.170, Y = -0.165, Z = -18.783, and dimensions (in Angstroms) X = 67.794, Y = 58.369, Z = 76.934. The three-dimensional and two-dimensional interactions of the receptor-ligands were analyzed and visualized by the Discovery Studio Visualizer (v21.1.0.20298) software (Dassault Systèmes Biovia Corp.) (Pătruică et al. 2024).

Molecular dynamics simulation

Molecular dynamic simulations were conducted on compounds with better binding affinity and more hydrogen bonds, namely Arbutin, Ruscoponticoside C, and Striatisporolide A, and compared to Chloramphenicol and Ampicillioic acid. Molecular dynamics simulations were performed using YASARA (Yet Another Scientific Artificial Reality Application) software with the AMBER14 force field (Krieger and Vriend 2014). The simulation conditions were set to match physiological conditions (310K, pH 7.4, 1 atm, and 0.9% salt concentration) for 50 ns. The macro programs employed included MD_run for conducting the simulations and MD_analyze for evaluating the Root Mean Square Fluctuation (RMSF), Radius of Gyration (Rg), and Root Mean Square Deviation (RMSD).

Data analysis

The data from the bacterial inhibition zones were analyzed for differences in bacterial growth inhibition using one-way analysis of variance (ANOVA) with Tukey's

test as a post hoc test ($p<0.005$) using SPSS Software version 23.

RESULTS AND DISCUSSION

Antibacterial activity assay

The results, including the inhibition zone diameter (in mm) of various pathogenic bacteria exposed to different concentrations of the ethyl acetate extract from *D. angustifolia* root bark, with positive control (C+) and negative control (C-), are presented in Table 1 and Figure 2. The inhibitory capability of the ethyl acetate extract varied for each bacterium. The one-way ANOVA statistical test, a robust method for comparing means, revealed significant differences ($P<0.05$) in each bacterial test result across each treatment, positive control, and negative control. The Tukey test indicated different results for each bacterium across various concentrations. The inhibitory capability of the ethyl acetate extract from *D. angustifolia* root bark on the growth of *S. aureus* showed an increase from 5%, 25%, and 50% concentrations, with the 50% concentration being significantly different from the 5% and 25% concentrations. This indicates that while the extract exhibits inhibitory potential at higher concentrations, it is still below the positive control. The inhibitory capability against *E. faecalis* increased with concentration, showing significant differences at 5%, 25%, and 50% concentrations. In contrast, for *E. coli* and *S. typhi*, no significant differences were observed, although the inhibition zones expanded with higher concentrations.

Staphylococcus aureus and *E. faecalis* are Gram-positive bacteria frequently targeted in antibacterial research due to their ability to cause a range of human infections. *S. aureus* can cause bacteremia, skin and soft tissue infections, food poisoning, and endocarditis. It can also impact microbial balance by influencing the intestinal immune system or increasing bacterial translocation into the bloodstream (Liu et al. 2024). *E. faecalis* is a bacterial pathogen that can cause opportunistic infections and plays a crucial regulatory role in these conditions (Nappi 2024). *E. faecalis* infection causes DNA damage in intestinal epithelial cells through superoxide production (Nappi et al. 2023). Despite both being Gram-positive bacteria, the research reveals that ethyl acetate extract inhibits *S. aureus* growth more effectively than *E. faecalis*. This is due to metabolic adaptation, differences in cell wall structure, resistance mechanisms, cell wall permeability, and specific interactions of active compounds with molecular targets of these two types of bacteria. These factors together determine the differing sensitivity of the two Gram-positive bacteria to ethyl acetate extract.

Escherichia coli and *S. typhi* are Gram-negative bacteria that can also lead to various infections within the human body. *E. coli* is considered one of the most significant human pathogens, causing severe infections alongside other major bacterial foodborne agents such as *Salmonella* spp. and *Campylobacter* (Ramos et al. 2020). *Salmonella* can lead to both acute infections and persistent asymptomatic carriage, contributing to chronic inflammation and carcinogenesis; there is also a relationship between an increased risk of colon cancer and *Salmonella* infections (Zha et al. 2019).

Table 1. Results of in antibacterial activity assay of ethyl acetate extract from *D. angustifolia* root bark against bacteria

Bacteria	C+	C-	Extract concentration		
			5%	25%	50%
Staphylococcus aureus	21.1±0.2d	0.0±0.0a	10.9±0.1b	11.6±0.4b	13.3±0.5c
Enterococcus faecalis	27.9±0.2e	0.0±0.0a	6.9±0.1b	7.6±0.1c	8.3±0.4d
Escherichia coli	29.2±0.5c	0.0±0.0a	7.0±0.5b	7.8±0.4b	8.0±0.8b
Salmonella typhi	26.9±0.4c	0.0±0.0a	7.0±0.2b	7.7±0.7b	7.8±0.7b

Notes: C+: positive control (Chloramphenicol) and C-: negative control (DMSO). Different superscripts (a, b, c, d, e) in the same line indicate the significant differences ($p<0.05$)

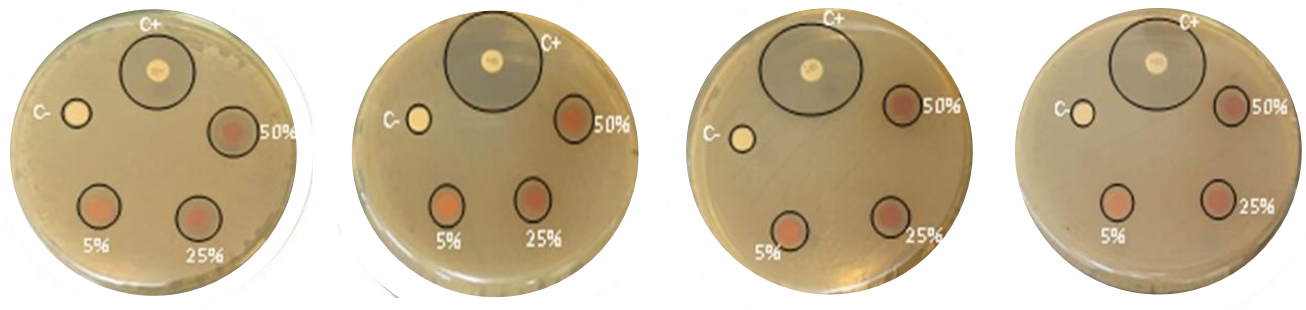

Figure 2. Diameter of the inhibition zone of antibacterial activity assay of ethyl acetate extract from A. *Staphylococcus aureus*; B. *Enterococcus faecalis*; C. *Escherichia coli*; D. *Salmonella typhi*

The results of this study indicate that the ethyl acetate extract is less effective in inhibiting the growth of *S. typhi* and *E. coli* than Gram-positive bacteria such as *S. aureus* and *E. faecalis*. The low effectiveness of ethyl acetate extract in inhibiting the growth of *E. coli* and *S. typhi* is due to the complex structure of Gram-negative cell walls, efficient efflux pump systems, enzyme production, and natural resistance mechanisms (Zhang and Cheng 2022). These factors make Gram-negative bacteria more resistant to various antimicrobial compounds, including those contained in ethyl acetate extract.

Gram-negative bacteria have an outer layer of lipopolysaccharides that serves as an additional barrier against the entry of antimicrobial compounds. This layer makes the cell wall of Gram-negative bacteria more impermeable compared to Gram-positive bacteria (Gauba and Rahman 2023). In addition to the LPS layer, Gram-negative bacteria have two cell membranes (an outer membrane and an inner membrane), which provide an additional protective layer, making it more challenging for active compounds to penetrate (Ghai 2023). Gram-negative bacteria often have more efficient efflux pump systems that can expel antimicrobial compounds from the cell before they reach lethal concentrations (Gaurav et al. 2023). These pumps reduce the effectiveness of many antibacterial agents, including compounds in ethyl acetate extracts.

Metabolite profiling of ethyl acetate of *D.angustifolia* root bark from LC-HRMS analysis

Based on the analysis of ethyl acetate extract from *D. angustifolia* root bark using LC-HRMS, the chromatogram in positive ion mode was obtained, as shown in Figure 3, and the compound annotation profiling is presented in Table 2. Table 2 presents the details of the retention time (Rt), area, annotated delta mass (ADM)/mass error, as well as the calculated molecular weight (CMW), observed mass-to-charge ratio mass spectra (MS), molecular formula (MF), annotated compounds, and groups of compounds. Structures of secondary metabolites identified based on the mass spectra were drawn using ChemDraw Profesional v16.0.1.4 software (Figure 4).

Table 2. Annotated compound of ethyl acetate extract from *D. angustifolia* root bark through LC-HRMS in positive ionization mode

Rt (minute)	Area (10^8)	ADM [ppm]	MS (m/z) $[M+H]^+$	CMW	Molecule formula	Annotated compound	Groups
0.81	0.13	0.32	127.04	126.03	$C_6H_6O_3$	Pyrogallol	Phenol
1.73	6.63	0.67	127.04	126.03	$C_6H_6O_3$	5-hydroxymethyl furfural	Furan
2.14	3.60	-1.79	143.03	142.03	$C_6H_6O_4$	Kojic acid	pyranone
2.26	6.93	-1.79	143.04	142.03	$C_6H_6O_4$	5-Hydroxymaltol	pyranone
2.37	2.6	0.18	127.04	126.03	$C_6H_6O_3$	Phloroglucinol	benzenetriol
5.58	0.16	-1.58	213.11	212.10	$C_{11}H_{16}O_4$	Striatisporolide A	Lactone
5.85	0.04	0.38	167.11	166.10	$C_{10}H_{14}O_2$	2,4,7-Decatrienoic acid	unsaturated fatty acid
6.24	0.18	0.45	151.07	150.07	$C_9H_{10}O_2$	4-Allylpyrocatechol	Phenylpropanoid
6.82	0.13	-0.11	179.07	178.06	$C_{10}H_{10}O_3$	4-Methoxycinnamic acid	Phenylpropanoid
7.62	0.34	-1.5	314.13	313.13	$C_{18}H_{19}NO_4$	Moupinamide	Alkaloid
8.51	1.21	0.52	111.04	110.04	$C_6H_6O_2$	Catechol	Phenolic
9.26	12.01	-1.92	181.12	180.11	$C_{11}H_{16}O_2$	5-Pentylresorcinol	Phenolic
9.30	1.01	-1.41	273.10	272.09	$C_{12}H_{16}O_7$	Arbutin	Phenolic glucoside
9.72	1.75	-1.43	221.19	220.18	$C_{15}H_{24}O$	Spathulenol	Sesquiterpenoid
9.79	0.22	-0.76	249.15	248.14	$C_{15}H_{20}O_3$	Reynosin	Sesquiterpenoid
10.39	0.14	-2.55	317.14	316.13	$C_{18}H_{20}O_5$	(2R)-7,30-dihydroxy-50,5-dimethoxy-8-methylflavan	Flavonoid
10.55	16.02	-2.04	445.29	444.29	$C_{27}H_{40}O_5$	Kammogenin	Steroidal saponin
10.58	1.32	-3.42	707.39	706.39	$C_{38}H_{58}O_{12}$	Ruscoponticoside C	Steroidal saponin
10.70	19.32	-2.56	447.31	446.30	$C_{27}H_{42}O_5$	Namogenin B	Steroid sapogenin
11.00	1.31	-2.04	445.29	444.29	$C_{27}H_{40}O_5$	Asparacosin A	Triterpenoid
11.20	1.89	-2.52	429.29	428.29	$C_{27}H_{40}O_4$	Neoruscogenin	steroidal saponin
11.95	2.19	-1.97	427.28	426.28	$C_{27}H_{38}O_4$	Azafrin	Carotenoid
12.13	7.75	-2.55	429.30	428.29	$C_{30}H_{52}O$	Cycloartanol	phytosterol
12.27	1.02	-1.58	203.18	202.17	$C_{15}H_{22}$	Cuparene	sesquiterpene
12.45	1.84	-2.24	193.16	192.15	$C_{13}H_{20}O$	β-ionone	Terpenoid
12.46	1.87	-2.96	205.19	204.19	$C_{15}H_{24}$	(E,E)-alpha-Farnesene	sesquiterpenoid
12.62	1.59	-1.58	203.18	202.17	$C_{15}H_{22}$	S-Curcumene	Terpenoid
12.67	2.06	-1.48	279.34	278.22	$C_{18}H_{30}O_2$	α-Eleostearic acid	Fatty acid
12.84	14.38	-2.35	431.31	430.31	$C_{27}H_{42}O_4$	Pennogenin	Spirostanol diglycosides
13.03	1.10	-1.83	217.16	216.15	$C_{15}H_{20}O$	(+)-ar-Turmerone	sesquiterpene
13.08	2.77	-1.09	295.23	294.22	$C_{18}H_{30}O_3$	9-OxoODE	oxylipin
13.16	2.20	-1.34	221.19	220.18	$C_{15}H_{24}O$	(-)-Caryophyllene oxide	Terpenoid
13.31	1.78	-1.45	221.19	220.18	$C_{15}H_{24}O$	Farnesal	seskuiterpena
14.26	2.06	-2.28	355.28	354.28	$C_{21}H_{38}O_4$	1-Linoleoyl glycerol	fatty acid glycerol
14.90	1.11	-0.92	282.27	281.27	$C_{18}H_{35}NO$	Oleamide	Amide fatty acid
16.31	0.95	-1.09	311.24	310.23	$C_{22}H_{30}O$	14'-apo-beta-carotenal	Terpenoid
18.44	2.59	-2.14	417.31	416.31	$C_{11}H_{18}O$	beta-Apo-8'-carotenal	Caretonoid

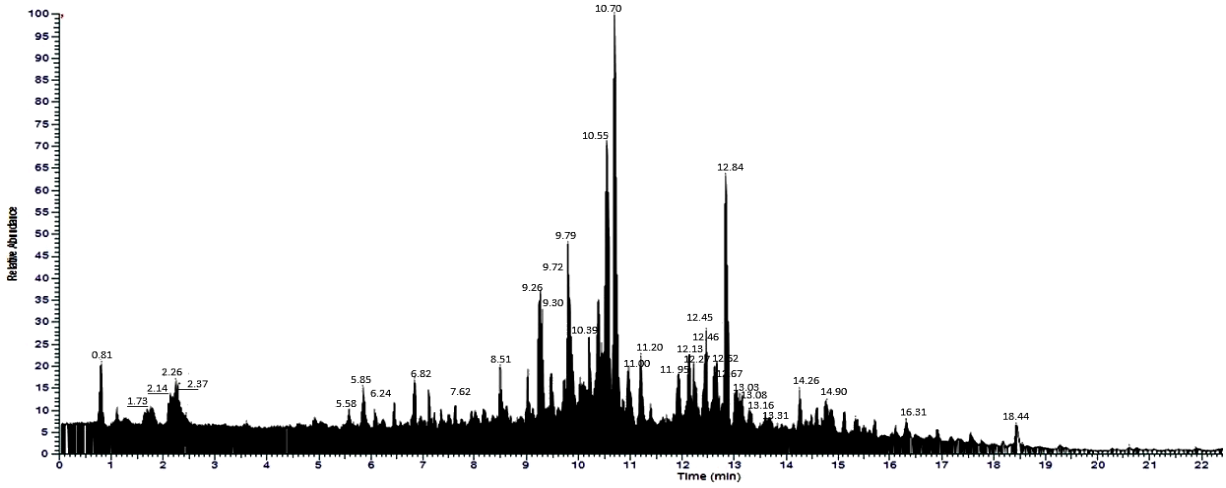

Figure 3. The chromatogram in positive ion mode of ethyl acetate extract from *D. angustifolia* root bark

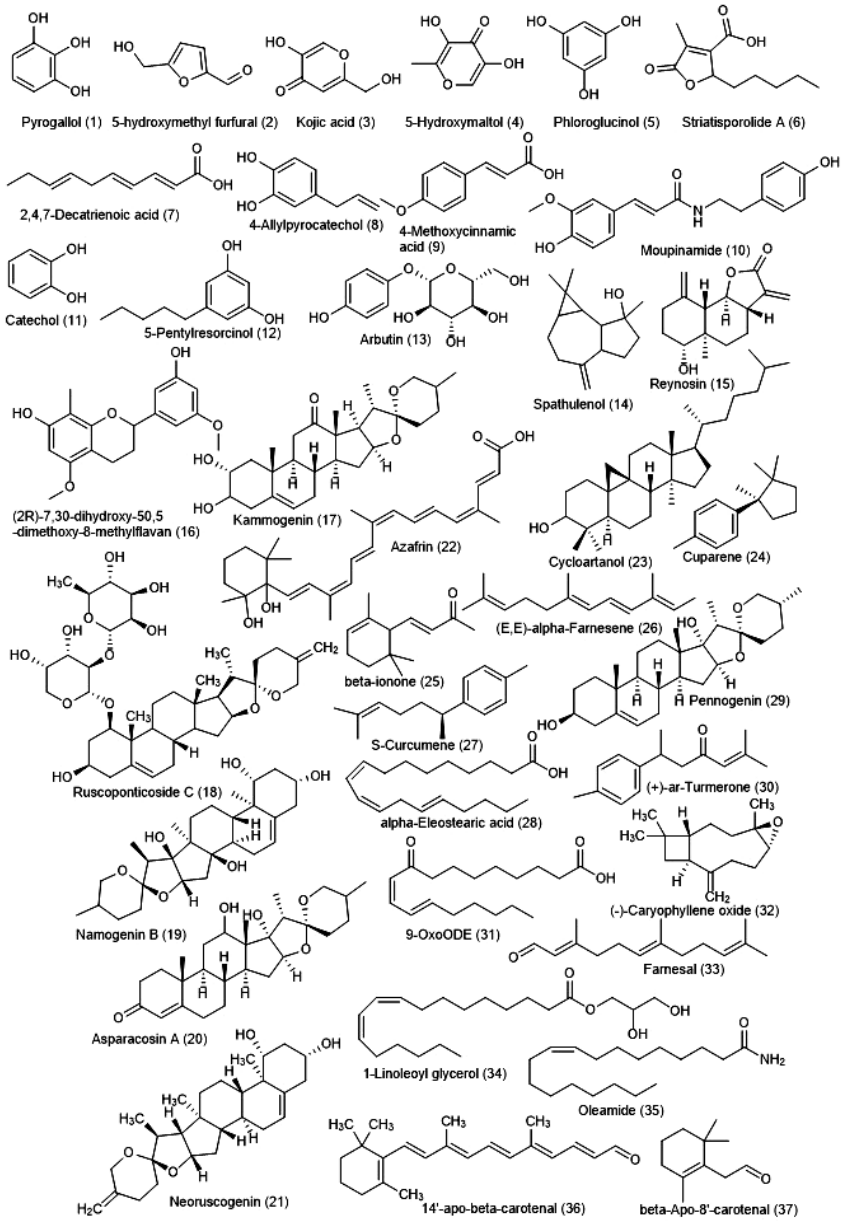

Figure 4. ChemDraw structures of secondary metabolites identified in ethyl acetate extract from *D. angustifolia* root bark

As shown in Table 2, there are thirty-seven annotated compounds present in the ethyl acetate extract from *D. angustifolia* root bark. These metabolites belong to the following groups of natural products: phenolics, furans, pyranones, lactones, fatty acids, phenylpropanoids, alkaloids, phenolic glucosides, terpenoids, flavonoids, steroidal saponins, carotenoids, and sterols. In this study, the ability of the ethyl acetate extract from *D. angustifolia* root bark to inhibit bacterial growth is certainly related to its phytochemical content, which includes phenolics, flavonoids, alkaloids, terpenoids, and saponins. Phenolic compounds have a versatile structure that accommodates a wide variety of chemical modifications, and they exhibit strong antimicrobial activities that can be significantly enhanced through functionalization. By interfering with bacterial cell wall synthesis, DNA replication, or enzyme production, phenolics can target multiple sites within bacteria. This targeting leads to an increased sensitivity of bacterial cells to these natural compounds, meaning that the bacteria become more susceptible to the antimicrobial effects of the phenolic compounds (Lobiuc et al. 2023). Flavonoids infiltrate cell walls, disrupt bacterial cell permeability, and lead to the breakdown of microsomes and lysosomes (Purwantiningsih et al. 2023). Flavonoids are generally less effective against Gram-negative bacteria but exhibit greater efficacy against Gram-positive species (Yan et al. 2024), contributing to greater inhibition of Gram-positive bacteria observed in this study. Alkaloids act as antibacterial agents by inhibiting bacterial cell wall synthesis, altering cell membrane permeability, disrupting bacterial metabolism, and hindering the synthesis of nucleic acids and proteins (Yan et al. 2021). Terpenoids exert antimicrobial effects through five primary mechanisms: disrupting cell membranes, interfering with quorum sensing (QS), inhibiting ATP and related enzymes, blocking protein synthesis, and producing synergistic effects (Huang et al. 2022). Saponins can alter cell membrane morphology and compromise their integrity while also synergistically enhancing the antimicrobial activity of traditional antibiotics by increasing membrane permeability and inhibiting biofilm synthesis; these effects are crucial for developing new therapies to combat antibiotic resistance (Li and Monje-Galvan 2023). Lactone can exert its antibacterial effect by damaging bacterial cell membranes and interfering with DNA function (Mazur and Masłowiec 2022).

Target prediction and docking analysis

Artificial intelligence-driven predictions of biological activity have become a common preliminary step in drug discovery. These virtual and computer-aided methods can be valuable in analyzing natural crude extracts (Singh et al. 2020). The annotated compounds (1-37) of the ethyl acetate extract from *D. angustifolia* root bark were analyzed using the prediction software PASS, which has shown high accuracy in its predictions, especially for those with a probability greater than Pa = 0.5 (Abdelgawad et al. 2022). As depicted in Figure 5, only compounds 6, 13, 18, and 32 stand out, achieving Pa scores greater than 0.5 for antibacterial activity. This potential is further explored in the docking analysis, where the four compounds were compared with the native ligand Ampicillioic acid (Ampicillin) and the drug Chloramphenicol, with the results detailed in Table 3 and Figure 6.

Table 3. Docking results of the ligand with the target protein 3HUN

Compound/native ligand	Binding energy (kcal/mol)	RMSD (refine unit)	H-bonding distance (Å)	Interacting residues
Arbutin	-6.0	1.161	Arg186(4.87), Glu114(4.83), Ser116(3.77)	Van der waals: Glu183, Ser263, Asn72, Ala182, Gly181, Ala74, Asn141, Ser75, Ser262, Gly261, Ser139, Phe241, Asp264, Leu115
(-)-Caryophyllene oxide	-5.3	1.919	Lys249(4.30)	Van der Waals: Thr240, Gly247 Pi-Alkyl: Ala230, Tyr239, Leu229, Ala248, Phe243
Ruscoponticoside C	-9.5	1.969	Gln60(4.61), Gln314(4.77,4.24,4.34), Leu61(5.88), Pro366(6.07), Ser27(3.36), Tyr315(6.94)	van der Waals: Tyr365, Asp346, Ser345, Sp313, Tyr63, Gln64, Asn26, Sp28, Leu62, Glu368, Arg367 Pi-alkyl: Phe347, Pro344
Striatisporolide A	-5.6	1.848	Arg186,Ser75(2.38), Thr180	van der Waals: Asn72, Glu183, Ser263, Glu114, Tyr291, Asn141, Ser116, Lys78, Gly181, Ser262, Ala182
Chloramphenicol	-5.6	1.325	Ser262(2.65,3.73,3.51), Ser75(3.83)	van der Waals: Tyr268, Glu114, Tyr291, Leu115, Tyr291, Ser263, Ser116, Gly261, Ser139 Phi-phi: Phe241
Ampicillioic acid	-6.9	1.430	Gln60(5.03), Tyr315(5.68), Leu61(5.04), Glu368(4.79), Leu62(6.04), Gln64(3.54)	van der Waals: Pro366, Tyr365, Arg367, Ser27, Tyr63, Phe347 Phi- Alkyl: Pro344

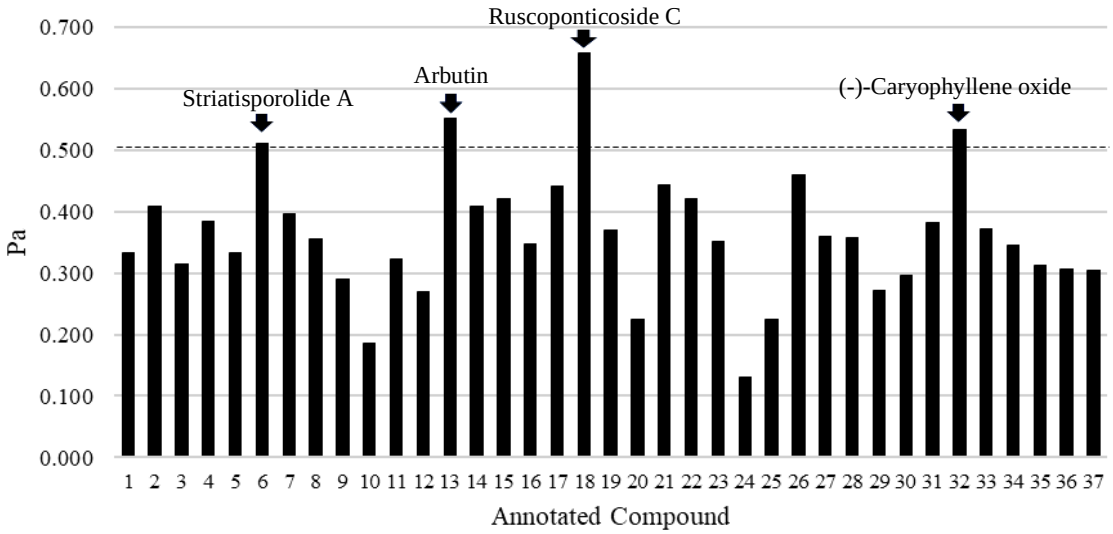

Figure 5. PASS prediction scores of the compounds 1-37 as antibacterial agents. Pa > 0.5 indicates a high probability of being active in vitro

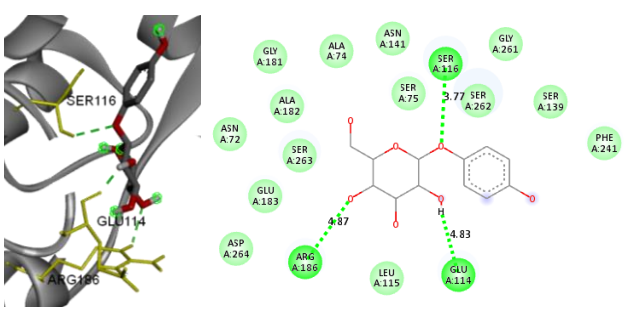

Arbutin

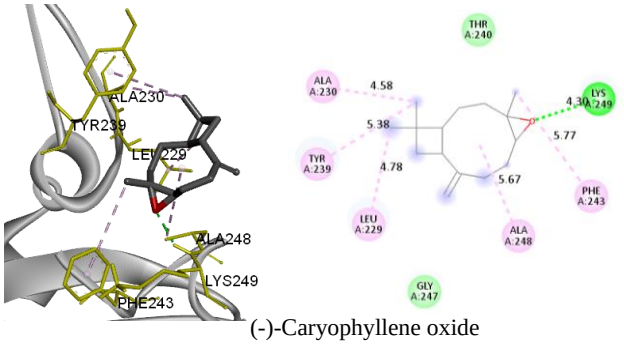

(-)-Caryophyllene oxide

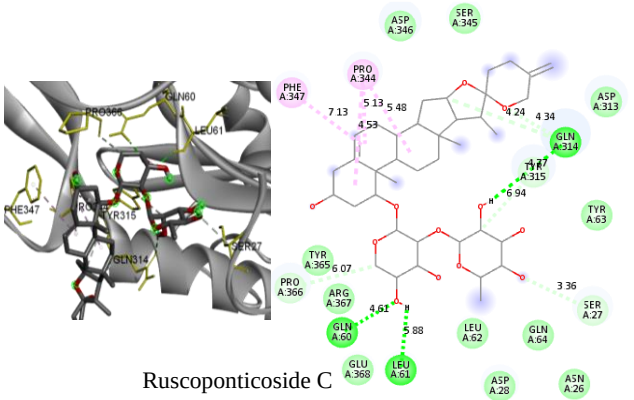

Ruscoponticoside C

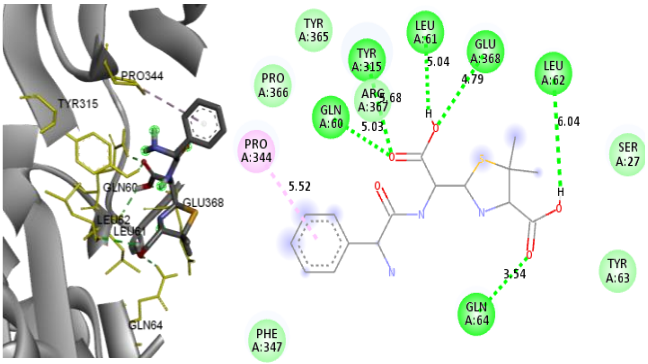

Ampicillioic acid (native ligand)

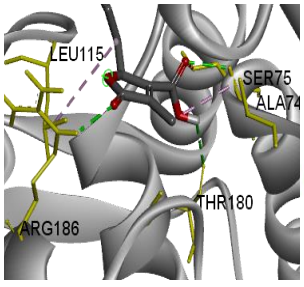

Striatisporolide A

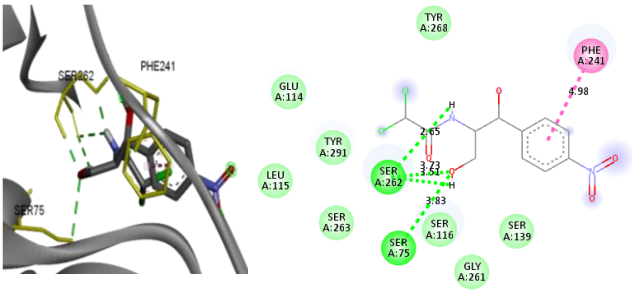

Chloramphenicol

Figure 6. Three-dimensional representation dan two-dimensional diagram of docking interaction of compounds/native ligand with 3HUN

Molecular docking is designed to simulate the interaction between ligand and protein molecules, assessing the ligand's binding activity by measuring its binding affinity (Sibero et al. 2022). Protein with PDB ID 3HUN is the crystal structure of Penicillin Binding Protein 4 (PBPs) from *S. aureus* bound with Ampicillin. PBPs are membrane-associated proteins that catalyze the final steps of murein biosynthesis, essential for forming and maintaining the bacterial cell wall. PBPs function as transpeptidases, carboxypeptidases, or, in some cases, transglycosylases. Beta-lactam antibiotics, such as penicillin, inhibit PBPs by competing to bind to the active site of these enzymes. Figure 6 visualizes the interaction of each compound with the target protein, aiding in the evaluation of their inhibitory potential against the target protein 3HUN in *S. aureus*. This analysis is crucial for developing new drugs that are effective against infections caused by these bacteria. In molecular docking, the most important factor for molecular activity is the binding affinity between the ligand and the target protein (Salamat et al. 2024). Molecular docking is a rapid method used to estimate the binding pose of a specific compound or ligand within a target protein and to predict binding affinity (Yang et al. 2022). More negative values indicate stronger binding and greater stability of the complex (Ravikumar et al. 2023). According to Table 3**,** Ruscoponticoside C shows lower binding energy (-9.5 kcal/mol) compared to Arbutin (-6.0 kcal/mol), (-)-Caryophyllene oxide (-5.3 kcal/mol), Striatisporolide A (-5.6 kcal/mol), including antibiotics Chloramphenicol (-5.6 kcal/mol) and the native ligand Ampicillioic Acid (-6.9 kcal/mol). This suggests that the compound exhibits the highest potential as an inhibitor of the 3HUN protein, demonstrating a strong binding affinity. These results align with consistent findings from the PASSonline analysis regarding the potential of Ruscoponticoside C as an antibacterial agent (Pa=0.656), which is higher compared to other compounds present in the ethyl acetate extract from *D. angustifolia* root bark (Figure 5).

Besides binding energy, residue interactions within the target protein also provide insights into the potential of ligands or compounds as antibacterial agents. The unique aspect of our research lies in the maps showing the strength and frequency between each amino acid residue and ligand functional groups, present a promising opportunity for developing new drug-design strategies and identifying drug selectivity and affinity (Madushanka et al. 2023). Figure 6 shows three-dimensional representations and two-dimensional diagrams of the interactions of these compounds with the 3HUN protein. Arbutin demonstrates significant interactions with residues Arg186, Glu114, and Ser116 through hydrogen bonds and several van der Waals interactions with other surrounding residues. (-)-Caryophyllene oxide forms hydrogen bonds with Lys249, van der Waals interactions with Thr240 and Gly247, and Pi-Alkyl interactions with several other residues. Ruscoponticoside C displays hydrogen bonds and complex van der Waals interactions, indicating a highly stable interaction with the target protein. Striatisporolide A interacts with residues Arg186, Ser75, and Thr180 through hydrogen bonds and several van der Waals interactions. Chloramphenicol forms hydrogen bonds with residues Ser262 and Ser75, along with several significant van der Waals interactions. Ampicillioic acid, as the native ligand, demonstrates strong and complex interactions with various protein residues, explaining its high binding affinity.

Hydrogen bonding, van der Waals interactions, and Pi-Alkyl interactions significantly contribute to the high affinity (Pantsar and Poso 2018). The higher binding affinity of Ruscoponticoside C compared to other compounds is primarily due to its abundance and variety of strong molecular interactions with the amino acid residues of the 3HUN protein. Ruscoponticoside C forms numerous hydrogen bonds with target residues, including Gln60, Gln314, Leu61, Pro366, Ser27, and Tyr315. These hydrogen bonds are highly stable and strong, significantly contributing to the low binding energy. Numerous van der Waals interactions with residues such as Tyr365, Asp346, Ser345, Sp313, Tyr63, Gln64, Asn26, Sp28, Leu62, Glu368, and Arg367 indicate that Ruscoponticoside C has extensive and stable contact with the target protein surface. These interactions help reinforce the overall binding between the ligand and the protein. The presence of Pi-Alkyl interactions with Phe347 and Pro344 further enhances the stability of the ligand-protein complex, as these interactions contribute an additional dimension of stabilization through aromatic stacking and alkyl interactions. Residues such as Gln60, Gln314, and Pro366 may be strategically located within or near the active site of the protein, allowing Ruscoponticoside C to disrupt protein function effectively. Interactions with these residues can lead to conformational changes in the protein or inhibit its catalytic activity, which is crucial for inhibiting bacterial function. The large number of hydrogen bonds and van der Waals interactions distribute the binding energy widely across the protein-ligand molecule, reducing the likelihood of dissociation and enhancing overall stability.

The binding affinity of Ruscoponticoside C is stronger compared to Chloramphenicol (a drug) and Ampicillioic acid (the native ligand). This indicates that Ruscoponticoside C is likely to form a more stable complex with the target protein. Ruscoponticoside C forms more hydrogen bonds with various residues on the target protein at varying distances, demonstrating stronger hydrogen interactions compared to Chloramphenicol. Although Chloramphenicol forms hydrogen bonds shorter than 3.5 Å (Ser262 at 2.65 Å), the number of these bonds is fewer. Both Ruscoponticoside C and Ampicillioic acid form hydrogen bonds with similar residues (Gln60, Leu61, Tyr315), but the hydrogen bond distances in Ruscoponticoside C tend to be more varied and shorter (Ser27 at 3.36 Å), indicating stronger and more stable hydrogen interactions. Shorter bond lengths (<3.5 Å) generally indicate stronger and more stable interactions (Channar et al. 2017). Van der Waals and pi-alkyl/pi-pi interactions play a significant role in the stability of the ligand-protein complex. These interactions, although weaker than hydrogen bonds, can significantly contribute to the overall binding affinity (Aziz et al. 2022). Ruscoponticoside C has more van der Waals and Pi-Alkyl interactions, suggesting a broader and more complex binding potential compared to Ampicillioic Acid. Extensive van der

Waals interactions indicate widespread contact with the protein surface, enhancing binding stability. The presence of Pi-Alkyl interactions with Phe347 and Pro344 indicates that the compound interacts with the aromatic or alkyl domains of the protein, which can strengthen the binding affinity.

Molecular dynamics simulation

Based on docking, three of the most potent compounds were selected for further molecular dynamics analysis (Arbutin, Ruscoponticoside C, and Striatisporolide A). These were then compared with the native ligand (Ampicillioic acid) and commonly used drugs (Chloramphenicol). Simulations using molecular dynamics were conducted to evaluate the stability of the interactions between the ligands and the protein (Rollando et al. 2023). The four parameters used in this simulation were the RMSD of the protein backbone and ligand movement, RMSF, and radius of gyration (Rg) (Figure 7). RMSD assesses the average deviation of protein backbone atom positions relative to a reference structure, typically the initial one. Lower RMSD values suggest that the ligand helps maintain the protein's structural stability. At the same time, a substantial increase in RMSD indicates major conformational changes, potentially pointing to less stable interactions or structural instability (Kurniawan and Ishida 2022). The RMSD of ligand movement reflects the stability of ligands during their interaction with proteins. A stable ligand exhibits minimal movement throughout the simulation, as reflected by a consistent RMSD value for its movement (Widyananda et al. 2022). Figure 7.A illustrates that chloramphenicol induces protein destabilization, evidenced by a fluctuating graph, which results in the interaction with the target protein. However, the protein structure stabilizes again between 30 and 50 ns. Arbutin, Striatisporolide A, and Ampicillioic acid contribute to the stability of the target protein, indicated by RMSD values below 3 Å. Ruscoponticoside C disrupts the protein's stability between 45.1 and 50 ns. Chloramphenicol interacts differently compared to the other compounds. Similarly, Figure 7.B shows that chloramphenicol exhibits more significant ligand movement between 6.5 and 31.5 ns before stabilizing in the following minutes. In contrast, the other four compounds demonstrate stable ligand movement, resulting in strong receptor binding and enhanced stability of the target protein structure. Low and stable RMSD values indicate that the ligand is tightly bound at the target protein's binding site, with little to no significant movement. The more fluctuating movement of chloramphenicol as a ligand causes receptor destabilization.

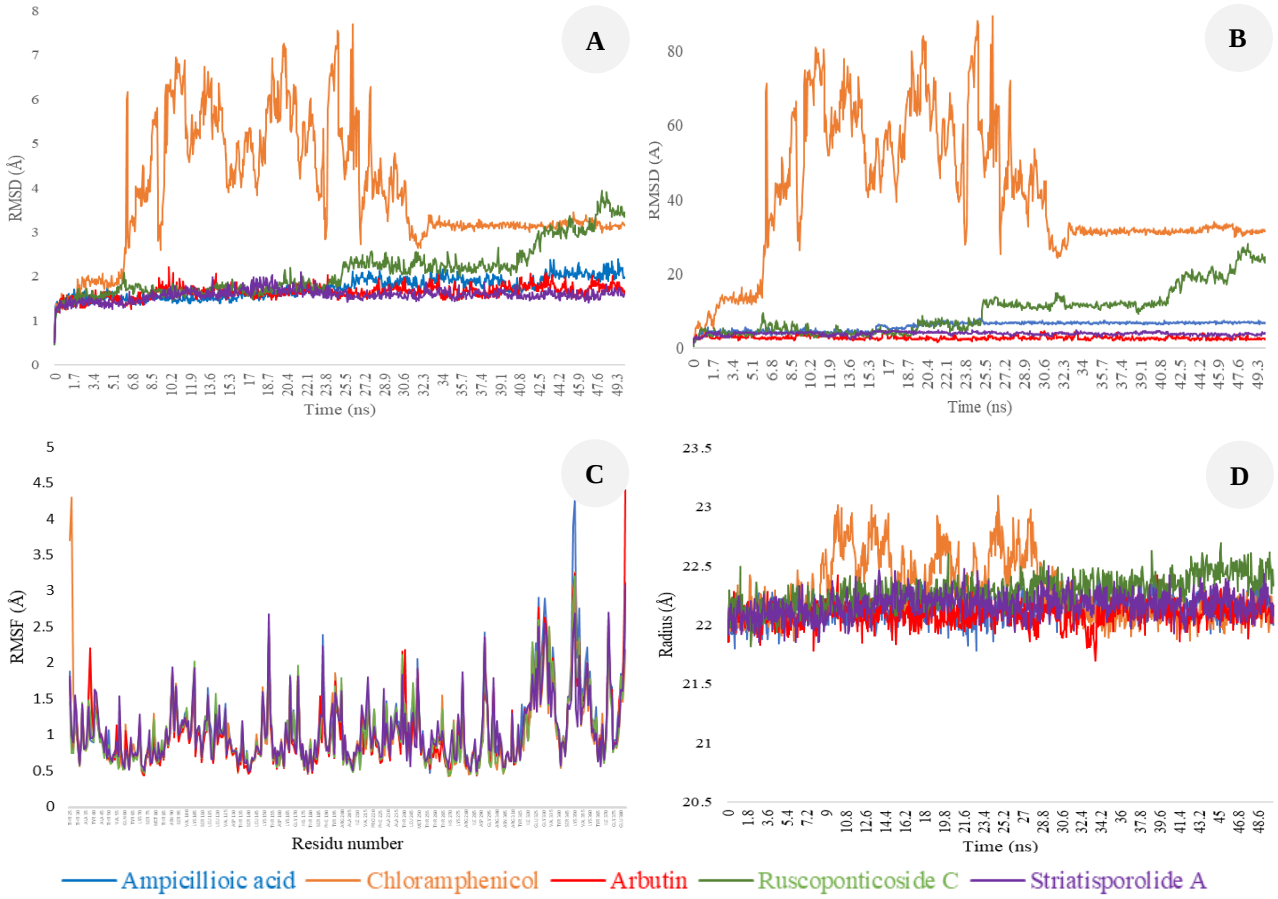

Figure 7. Molecular Dynamic A. RMSD the protein backbone; B. RMSD ligand movement; C. RMSF; D. Radius of gyration of the solute/Rg of 3HUN with ligands. Line color note: Ampicillioic acid (blue), Chloramphenicol (orange), Arbutin (red), Ruscoponticoside C (green), and Striatisporolide A (purple)

RMSF is a parameter used to measure the flexibility of amino acid residues in a protein during molecular dynamics simulations. A higher RMSF value indicates greater flexibility or movement of the residue during the simulation, while a lower value suggests increased stability or reduced mobility (Bagewadi et al. 2023). Figure 7.C illustrates the fluctuating interactions between each ligand and the residues. Most residues remain below 2.5 Å, indicating that the majority of the receptor structure remains stable (Fatriansyah et al. 2022). This suggests that these ligands interact well, although certain areas of the receptor continue to exhibit high flexibility. Ampicillioic acid, as the native ligand, shows instability with amino acid residues Arg327, Lys331, Lys350, Lys372, Lys353, Lys349, Asp351, and Gln383. Chloramphenicol exhibits fluctuating interactions with Asn26, Lys331, Lys350, Lys349, and Thr25. Arbutin is more flexible with Lys350, Lys372, Lys349, His382, and Gln383. Ruscoponticoside C is unstable with Arg327, Lys350, Gln383, and Lys349. Striatisporolide A shows significant movement with residues Lys350, Lys153, Lys372, and Gln383. The Arbutin ligand displays a relatively stable RMSF profile, with most residues showing low fluctuations between 0.5 and 1.5 Å. Despite a few peaks exceeding 2.5 Å, the receptor's overall fluctuations with Arbutin are relatively low, indicating stable interactions. The ligands Ruscoponticoside C and Striatisporolide A exhibit fluctuations, suggesting that some residues experience greater movement; however, most residues remain stable with fluctuations below 2.5 Å. Ampicillioic acid has a more fluctuating RMSF profile compared to the other compounds, though its residues are not involved in the inhibitor's active site.

The radius of gyration (Rg) indicates the overall size of a chain molecule; it is used to evaluate the extent of structural changes in a protein during molecular dynamics (MD) simulations (Ghahremanian et al. 2022). An increased Rg suggests a more extended conformation, while a decreased Rg indicates a more compact structure. Therefore, a significant fluctuation in Rg could indicate protein instability (Ravikumar et al. 2023). The average Rg values from 0 to 50 ns for the 3HUN protein with the ligands Ampicillioic acid, Chloramphenicol, Arbutin, Ruscoponticoside C, and Striatisporolide A were 22.13±0.10 Å, 22.29±0.26 Å, 22.09±0.10 Å, 22.28±0.13 Å, and 22.16±0.10 Å, respectively. Figure 7.D depicts the stability of the receptor-ligand complex structure throughout the simulation. Chloramphenicol exhibits a more fluctuating Rg compared to the other compounds, indicating that the complex undergoes significant conformational changes, which may suggest less stable interactions. The Rg value starts to fluctuate from 8.1 ns to 30 ns and then remains constant. Ligands Arbutin, Ruscoponticoside C, and Striatisporolide A exhibit Rg plots similar to that of the native ligand Ampicillioic acid; Ligands or compounds with the most stable Rg and low fluctuations are capable of forming stable complexes, which is often associated with higher biological effectiveness.

In conclusion, the ethyl acetate extract from *D. angustifolia* root bark exhibited better antibacterial potential against Gram-positive bacteria compared to Gram-negative bacteria. Among the 37 annotated compounds with PASS prediction, four (Arbutin, (-)-Caryophyllene oxide, Ruscoponticoside C, and Striatisporolide A) showed potential as antibacterial agents (Pa >0.5). Molecular docking analysis revealed that these four compounds had varying interactions with the target protein 3HUN. Ruscoponticoside C exhibited a similar amino acid residue binding to the native ligand Ampicillioic acid. Molecular dynamics simulation indicated that Chloramphenicol demonstrated fluctuating stability with the 3HUN receptor protein compared to the other compounds. Further research should focus on the purification and isolation of compounds of the ethyl acetate extract from *D. angustifolia* root bark, as well as exploring additional bioactivity potentials and conducting *in vivo* or clinical testing.

ACKNOWLEDGEMENTS

This research was supported by a grant from the Indonesian Ministry of Education, Culture, Research, and Technology through Doctoral Dissertation Research (*Penelitian Disertasi Doktor*) with contract No. 045/E5/PG.02.00.PL/2024. The authors would like to thank the Biocomputation and Bioinformatics Laboratory, Biology Department, Faculty of Science and Mathematics, Universitas Brawijaya, Malang, Indonesia.The authors also thank Prof. Widodo, for providing YASARA license and AI-Center UB for High Performance Computer (HPC) facilities.

REFERENCES

Abdallah EM, Alhatlani BY, de Paula Menezes R, Martins CHG. 2023. Back to nature: Medicinal plants as promising sources for antibacterial drugs in the post-antibiotic era. Plants 12 (17): 3077. DOI: 10.3390/plants12173077.

Abdelgawad MA, Hamed AA, Nayl AA, Badawy MSEM, Ghoneim MM, Sayed AM, Hassan HM, Gamaleldin NM. 2022. The chemical profiling, docking study, and antimicrobial and antibiofilmactivities of the endophytic fungi *Aspergillus* sp. AP5. Molecules 24 (5): 1704. DOI: 10.3390/ molecules27051704.

Aryal B, Adhikari B, Aryal N, Bhattarai BR, Khadayat K, Parajuli N. 2021. LC-HRMS profiling and antidiabetic, antioxidant, and antibacterial activities of *Acacia catechu* (L.f.) Willd. Biomed Res Intl 2021: 7588711. DOI: 10.1155/2021/7588711.

Aziz M, Ejaz SA, Zargar S, Akhtar N, Aborode AT, Wani TA, Batiha GE, Siddique F, Alqarni M, Akintola AA. 2022. Deep learning and structure-based virtual screening for drug discovery against NEK7: A novel target for the treatment of cancer. Molecules 27 (13): 4098. DOI: 10.3390/molecules27134098.

Babu K, Prabhu DS. 2024. *Dracaena trifasciata* (Prain) Mabb traditional use, pharmacognosy, phytochemistry, and pharmacology : A comprehensive review. J Phytopharm 13 (3): 235-241. DOI: 10.31254/phyto.2024.13307.

Bagewadi ZK, Yunus Khan TM, Gangadharappa B, Kamalapurkar A, Mohamed Shamsudeen S, Yaraguppi DA. 2023. Molecular dynamics and simulation analysis against superoxide dismutase (SOD) target of *Micrococcus luteus* with secondary metabolites from *Bacillus licheniformis* recognized by genome mining approach. Saudi J Biol Sci 30: 103753. DOI: 10.1016/j.sjbs.2023.103753.

Balouiri M, Sadiki M, Ibnsouda SK. 2016. Methods for *in vitro* evaluating antimicrobial activity: A review. J Pharm Anal 6 (2): 71-79. DOI: 10.1016/j.jpha.2015.11.005.

Banskota AH, Tezuka Y, Tran QL, Kadota S. 2003. Chemical constituents and biological activities of Vietnamese medicinal plants. Curr Top Med Chem 3: 227-248. DOI: 10.2174/1568026033392516.

Barua I, Sonowal R. 2011. Indigenous herbal medicine among the Sonowal Kachari tribe : A study in a forest village in Dibrugarh, Assam, India. NeBIO 2 (4): 31-35.

Breijyeh Z, Karaman R. 2023. Design and synthesis of novel antimicrobial agents. Antibiotics 12: 628. DOI: 10.3390/antibiotics12030628.

Campos L, Seixas L, Dias S, Peres AM, Veloso ACA, Henriques M. 2022. effect of extraction method on the bioactive composition, antimicrobial activity, and phytotoxicity of pomegranate by-products. Foods 11 (7): 992. DOI: 10.3390/foods11070992.

Channar PA, Saeed A, Albericio F, Larik FA, Abbas Q, Hassan M, Raza H, Seo SY. 2017. Sulfonamide-Linked ciprofloxacin, sulfadiazine and amantadine derivatives as a novel class of inhibitors of jack bean urease; synthesis, kinetic mechanism and molecular docking. Molecules 22 (8): 1352. DOI: 10.3390/molecules22081352.

Dewatisari WF, To'bungan N. 2024. Review: Phytochemistry and ethnopharmacology of *Dracaena trifasciata*. Nusantara Biosci 16: 169-184. DOI: 10.13057/nusbiosci/n160203.

Dutta M, Barooah MS. 2021. Consumption and utilisation of indigenous herbal plants among the Sonowal Kachari Tribes of Assam -A Review. J Xi'an Univ Archit Technol XIII (7): 68-76.

Fadana Y, Dinana IA, Srihardyastutie A, Rollando R, Masruri M. 2023. Screening Indonesian pine (*Pinus merkusii* Jungh at de Vriese) Compound as an antibacterial agent: In vitro and in silico study. Trop J Nat Prod Res 7 (3): 2586-2595. DOI: 10.26538/tjnpr/v7i3.19.

Fatriansyah JF, Boanerges AG, Kurnianto SR, Pradana AF, Fadilah, Surip SN. 2022. Molecular dynamics simulation of ligands from *Anredera cordifolia* (Binahong) to the Main Protease (M pro) of SARS-CoV-2. J Trop Med 2022: 1178228. DOI: 10.1155/2022/1178228.

Gaona-López C, Méndez-Álvarez D, Moreno-Rodríguez A, Bautista-Martínez JL, De Fuentes-Vicente JA, Nogueda-Torres B, García-Torres I, López-Velázquez G, Rivera G. 2024. TATA-binding protein-based virtual screening of FDA drugs identified new anti-giardiasis agents. Intl J Mol Sci 25: 6238. DOI: 10.3390/ijms25116238.

Gauba A, Rahman KM. 2023. Evaluation of antibiotic resistance mechanisms in gram-negative bacteria. Antibiotics 12 (11): 1590. DOI: 10.3390/antibiotics12111590.

Gaurav A, Bakht P, Saini M, Pandey S, Pathania R. 2023. Role of bacterial efflux pumps in antibiotic resistance, virulence, and strategies to discover novel efflux pump inhibitors. Microbiology 169: 001333. DOI: 10.1099/mic.0.001333.

Ghahremanian S, Mehdi M, Raeisi K, Toghraie D. 2022. Molecular dynamics simulation approach for discovering potential inhibitors against SARS-CoV-2: A structural review. J Mol Liq 354: 118901. DOI: 10.1016/j.molliq.2022.118901.

Ghai I. 2023. A barrier to entry: examining the bacterial outer membrane and antibiotic resistance. Appl Sci 13: 4238. DOI: 10.3390/app13074238.

Ghalloo BA, Khan KUR, Ahmad S, Aati HY, Al-Qahtani J H, Ali B, Mukhtar I, Hussain M, Shahzad MN, Ahmed I. 2022. Phytochemical profiling, in vitro biological activities, and in silico molecular docking studies of *Dracaena reflexa*. Molecules 27 (3): 913. DOI: 10.3390/molecules27030913.

Hanh NT, Hop NV, Thai HV, Quy NV, Luong NT. 2021. Traditional knowledge about medicinal plants of Tay Ethnic Community in South Vietnam: A case study at Lan Tranh Protection Forest, Lam Dong Province. Intl J Prog Sci Technol 29 (1): 565-589. DOI: 10.52155/ijpsat.v29.1/3584.

Huang W, Li P, Liu Y, Huang W, Ju Y, Wang J, Ntumwel CB, Long C. 2016. Ethnobotanical study on medicinal plants used by Li people in Ledong, Hainan Island, China. Acta Soc Bot Pol 85 (1): 1-15. DOI: 10.5586/asbp.3485.

Huang W, Wang Y, Tian W, Cui X, Tu P, Li J, Shi S, Liu X. 2022. Biosynthesis investigations of terpenoid, alkaloid, and flavonoid antimicrobial agents derived from medicinal plants. Antibiotics 11 (10): 1380. DOI: 10.3390/antibiotics11101380.

Karta IW, Warsito W, Masruri M, Mudianta, IW. 2024. Effects of solvent polarity on phytoconstituents, antioxidant and anti-inflammatory activities of *Dracaena angustifolia* Roxb root bark extracts. Trop J Nat Prod Res 8 (5): 7148-7153. DOI: 10.26538/tjnpr/v8i5.15.

Krieger E, Vriend G. 2014. YASARA View-Molecular graphics for all devices - from smartphones to workstations. Bioinformatics 30 (20): 2981-2982. DOI: 10.1093/bioinformatics/btu426.

Kurniawan J, Ishida T. 2022. Protein model quality estimation using molecular dynamics simulation. ACS Omega 7 (28): 24274-24281. DOI: 10.1021/acsomega.2c01475.

Li J, Monje-Galvan V. 2023. In vitro and in silico studies of antimicrobial saponins: A review. Processes 11: 2856. DOI: 10.3390/pr11102856.

Liu A, Garrett S, Hong W, Zhang J. 2024. *Staphylococcus aureus* infections and human intestinal microbiota. Pathogens 13 (4): 276. DOI: 10.3390/pathogens13040276.

Lobiuc A, Pavăl NE, Mangalagiu II, Gheorghiță R, Teliban GC, Amăriucăi-Mantu D, Stoleru V. 2023. Future antimicrobials: Natural and functionalized phenolics. Molecules 28 (3): 1114. DOI: 10.3390/molecules28031114.

Madushanka A, Moura RT, Verma N, Kraka E. 2023. Quantum mechanical assessment of protein-ligand hydrogen bond strength patterns: Insights from semiempirical tight-binding and local vibrational mode theory. Intl J Mol Sci 24 (7): 6311. DOI: 10.3390/ijms24076311.

Masruri M, Wiryawan A, Ikhtiarini N, Nurravida E. 2024. Phytochemistry and antibacterial activity the water extract from *Paraserianthes falcataria*. Alchemy J Chem 12: 36-41. DOI: 10.18860/al.v12i1.24234.

Mazur M, Masłowiec D. 2022. Antimicrobial activity of lactones. Antibiotics 11 (10): 1327. DOI: 10.3390/antibiotics11101327.

Mendonça AMS, Monteiro CA, Moraes-Neto RN, Monteiro AS, Mondego-Oliveira R, Nascimento CEC, da Silva LCN, Lima-Neto LG, Carvalho RC, de Sousa EM. 2022. Ethyl acetate fraction of *Punica granatum* and its Galloyl-HHDP-Glucose compound, alone or in combination with fluconazole, have antifungal and antivirulence properties against *Candida* sp.. Antibiotics 11 (2): 265. DOI: 10.3390/antibiotics11020265.

Nappi F, Avtaar Singh SS, Jitendra V, Fiore A. 2023. Bridging molecular and clinical sciences to achieve the best treatment of Enterococ*cus faecalis* endocarditis. Microorganisms 11 (10): 2604. DOI: 10.3390/microorganisms11102604.

Nappi F. 2024. Current knowledge of Enterococcal Endocarditis: A disease lurking in plain sight of health providers. Pathogens 13 (3): 235. DOI: 10.3390/pathogens13030235.

Pantsar T, Poso A. 2018. Binding affinity via docking: Fact and fiction. Molecules 23 (8): 1899. DOI: 10.3390/molecules23081899.

Pătruică S, Adeiza SM, Hulea A, Alea E, Cocan I, Moraru D, Imbrea I, Floares D, Pet I, Imbrea F, Obistioiu D. 2024. Romanian bee product analysis: Chemical composition, antimicrobial activity, and molecular docking insights. Foods 13 (10): 1455. DOI: 10.3390/foods13101455.

Pinzi L, Rastelli G. 2019. Molecular docking: Shifting paradigms in drug discovery. Intl J Mol Sci 20 (18): 4331. DOI: 10.3390/ijms20184331.

Purwantiningsih TI, Widyobroto BP, Suranindyah YY, Artama WT. 2023. Antibacterial activity of faloak (*Sterculia quadrifida*) leaves extract. Biodiversitas 24 (12): 6613-6620. DOI: 10.13057/biodiv/d241223.

Ramata-Stunda A, Petrina Z, Valkovska V, Boroduškis M, Gibnere L, Gurkovska E, Nikolajeva V. 2022. Synergistic effect of polyphenol-rich complex of plant and green propolis extracts with antibiotics against respiratory infections causing bacteria. Antibiotics 11: 160. DOI: 10.3390/antibiotics11020160.

Ramos S, Silva V, de Lurdes Enes Dapkevicius M, Caniça M, Tejedor-Junco MT, Igrejas G, Poeta P. 2020. Escherichia coli as commensal and pathogenic bacteria among food-producing animals: Health implications of extended spectrum β-lactamase (ESBL) production. Animals 10: 2239. DOI: 10.3390/ani10122239.

Ravikumar Y, Koonyosying P, Srichairatanakool S, Ponpandian LN, Kumaravelu J, Srichairatanakool S. 2023. *In silico* molecular docking and dynamics simulation analysis of potential histone lysine methyl transferase inhibitors for managing β-thalassemia. Molecules 28 (21): 7266. DOI: 10.3390/molecules28217266.

Rollando R, Monica E, Afthoni MH, Warsito W, Masruri M, Widodo N, Zainul R. 2023. In-vitro and In-silico Studies of a phenylpropanoid compound isolated from *Sterculia quadrifida* Seeds and its inhibitory effect on matrix metalloproteinase-9. Trop J Nat Prod Res 7 (7): 3490-3495. DOI: 10.26538/tjnpr/v7i7.30.

Rustini R, Aisy DR, Putra PP, Andayani R, Dwinatrana K. 2023. Antibacterial activity of endophytic bacterial extracts isolated from Pineapple Peel (*Ananas comosus* L.). Trop J Nat Prod Res 7 (7): 3320-3324. DOI: 10.26538/tjnpr/v7i7.8.

Sakong P, Khampitak T, Cha U, Pinitsoontorn C, Sriboonlue P, Yongvanit P, Boonsiri P. 2011. Antioxidant activity and bioactive phytochemical contents of traditional medicinal plants in northeast Thailand. J Med Plants Res 5 (31): 6822-6831. DOI: 10.5897/JMPR11.1222.

Salamat A, Kosar N, Mohyuddin A, Imran M, Zahid MN, Mahmood T. 2024. SAR, molecular docking and molecular dynamic simulation of natural inhibitors against SARS-CoV-2 Mpro Spike Protein. Molecules 29 (5): 1144. DOI: 10.3390/molecules29051144.

Sasse M, Rainer M. 2022. Mass spectrometric methods for non-targeted screening of metabolites: A future perspective for the identification of unknown compounds in plant extracts. Separations 9 (12): 415. DOI: 10.3390/separations9120415.

Sibero MT, Pribadi R, Ambariyanto A, Haryanti D, Kharisma VD, Dewi AS, Patantis G, Zilda DS, Murwani R. 2022. Ethnomedicinal bioprospecting of *Rhizophora apiculata* leaves through *in silico* and *in vitro* approaches as antioxidant, α-glucosidase inhibitor and anticancer. Biodiversitas 23: 6437-6447. DOI: 10.13057/biodiv/d231242.

Singh AV, Rosenkranz D, Ansari MHD, Singh R, Kanase A, Singh SP, Johnston B, Tentschert J, Laux P, Luch A. 2020. Artificial intelligence and machine learning empower advanced biomedical material design to toxicity prediction. Adv Intell Syst 2 (12): 1-19. DOI: 10.1002/aisy.202000084.

Surayya L, Putri EKA, Malik C. 2016. Ethnobotanical study of herbal medicine in Ranggawulung Urban Forest, Subang District, West Java, Indonesia. Biodiversitas 17: 172-176. DOI: 10.13057/biodiv/d170125.

Thu ZM, Myo KK, Aung HT, Armijos C, Vidari G. 2020. Flavonoids and stilbenoids of the genera Dracaena and Sansevieria : structures and bioactivities. Molecules 25: 2608. DOI: 10.3390/molecules25112608.

Thu ZM, Oo SM, Nwe T M, Aung HT, Armijos C, Hussain FHS, Vidari G. 2021. Structures and bioactivities of steroidal saponins isolated from the genera *Dracaena* and *Sansevieria*. Molecules 26 (7):1916. DOI: 10.3390/molecules26071916.

Vaou N, Stavropoulou E, Voidarou C, Tsigalou C, Bezirtzoglou E. 2021. Towards advances in medicinal plant antimicrobial activity: A review study on challenges and future perspectives. Microorganisms 9 (10): 2041. DOI:10.3390/microorganisms9102041.

Villanueva ELC, Buot IE. 2020. Useful plants of the Alangan Mangyan of Halcon Range, Mindoro Island, Philippines. J Mar Isl Cult 9 (1): 76-102. DOI: 10.21463/jmic.2020.09.1.05.

Widyananda MH, Wicaksono ST, Rahmawati K, Puspitarini S, Ulfa SM, Jatmiko YD, Masruri M, Widodo N. 2022. A potential anticancer mechanism of finger root (*Boesenbergia rotunda*) extracts against a breast cancer cell line. Scientifica 2022: 9130252. DOI: 10.1155/2022/9130252

Yan Y, Li X, Zhang C, Lv L, Gao B, Li M. 2021. Research progress on antibacterial activities and mechanisms of natural alkaloids: A review. Antibiotics 10 (3): 318. DOI: 10.3390/antibiotics 10030318.

Yan Y, Xia X, Fatima A, Zhang L, Yuan G, Lian F, Wang Y. 2024. Antibacterial activity and mechanisms of plant flavonoids against gram-negative bacteria based on the antibacterial statistical model. Pharmaceuticals 17 (3): 292. DOI: 10.3390/ph17030292.

Yang C, Chen EA, Zhang Y. 2022. Protein-Ligand docking in the machine-learning era. Molecules 27 (14): 4568. DOI: 10.3390/molecules27144568.

Yi J, Zhao T, Zhang Y, Tan Y, Han X, Tang Y, Chen G. 2022. Isolated compounds from *Dracaena angustifolia* Roxb and acarbose synergistically / additively inhibit α - glucosidase and α - amylase: An *in vitro* study. BMC Complement Med Ther 22: 177. DOI: 10.1186/s12906-022-03649-3.

Zha L, Garrett S, Sun J. 2019. *Salmonella* infection in chronic inflammation and gastrointestinal cancer. Diseases 7: 28). DOI: 10.3390/diseases7010028.

Zhang F, Cheng W. 2022. The mechanism of bacterial resistance and potential bacteriostatic strategies. Antibiotics 11 (9): 1215. DOI: 10.3390/antibiotics11091215.